Supplementary figures

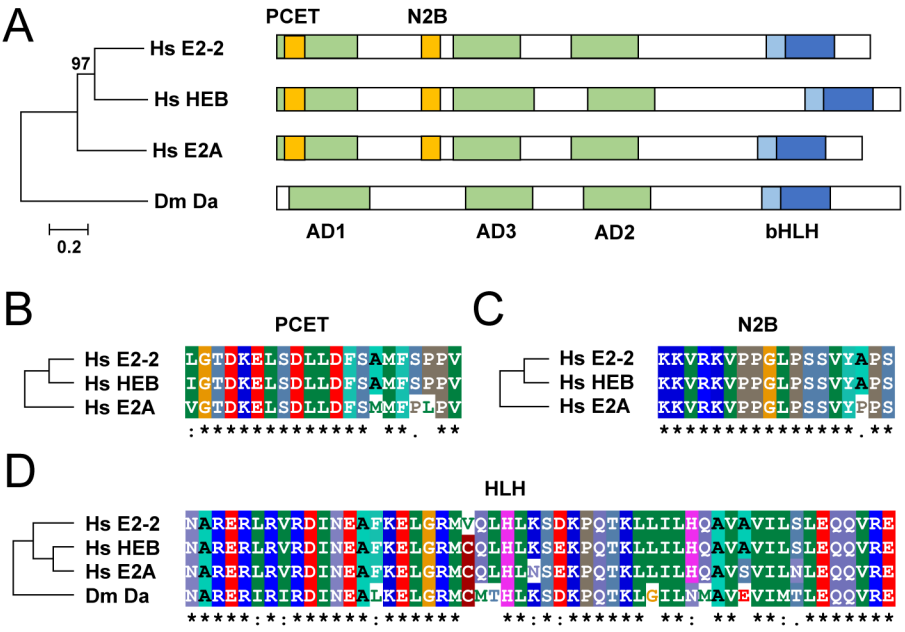

Fig. S1. Homology analysis of E2-2, HEB and E2A. (*A*) Phylogenetic tree constructed with full-length amino acid sequences of the human (*Hs*) E proteins and the sole fruit fly (*Dm*) homologue, Daughterless (Da). Also shown are their domain architectures, including the PCET (p300/CBP and ETO target) and N2B (NHR2-binding) motifs that directly interact with AML1-ETO. (*B* and *C*) Comparison of the PCET (*B*) and N2B (*C*) sequences in the three human E proteins. Note that E2-2 and HEB share high similarities in these two motifs, whereas E2A shows different amino acids. (*D*) Comparison of the HLH domains of the E proteins. Note that, unlike the cases of PCET and N2B, the HLH of E2-2 diverges from those of HEB and E2A.

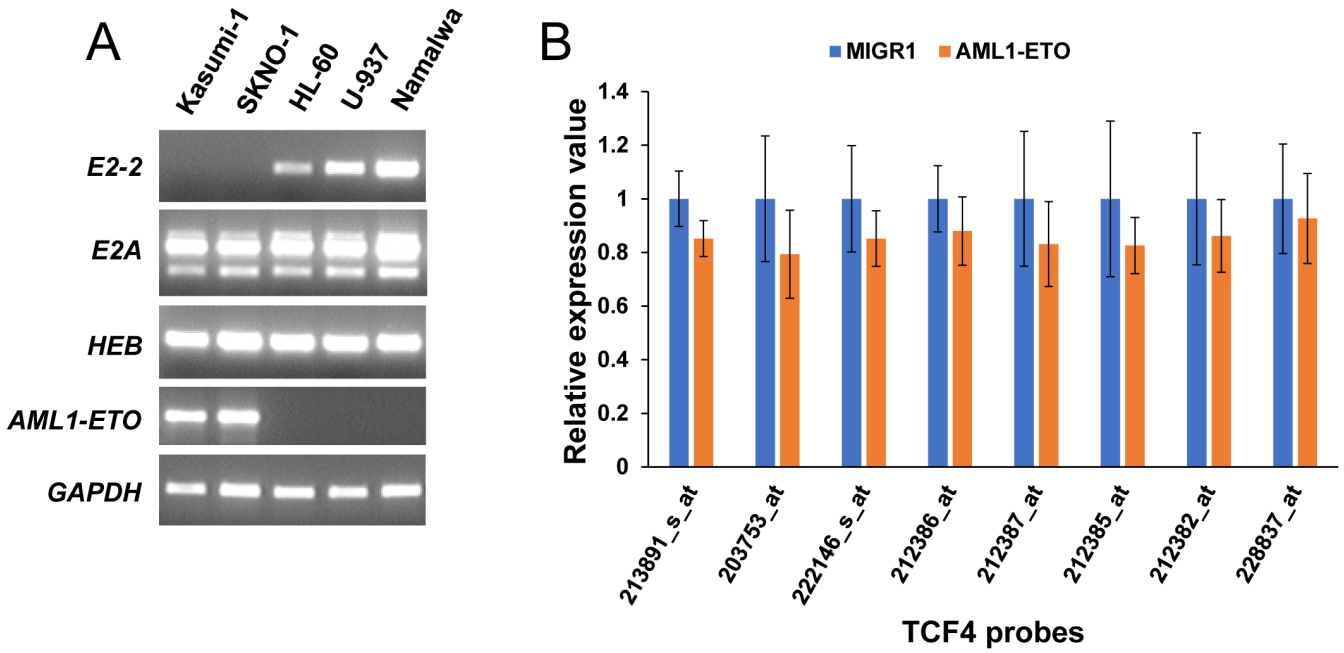

Fig. S2. Expression of *E2-2* in leukemic cell lines and in human CD34$^+$ HSPCs transduced with AML1-ETO. (*A*) RT-PCR analysis of E protein expression in different leukemic cell lines. Although the results overlap with those of Fig. 1B, this separate experiment includes an extra cell line, Namalwa. (*B*) Microarray data showing that ectopic expression of AML1-ETO in human CD34$^+$ cells does not significantly affect *TCF4*/*E2-2* expression. Each Affymetrix probe value is based on three independent infections of the cells with control vector (MIGR1) or AML1-ETO; none of these probes shows a significant difference.

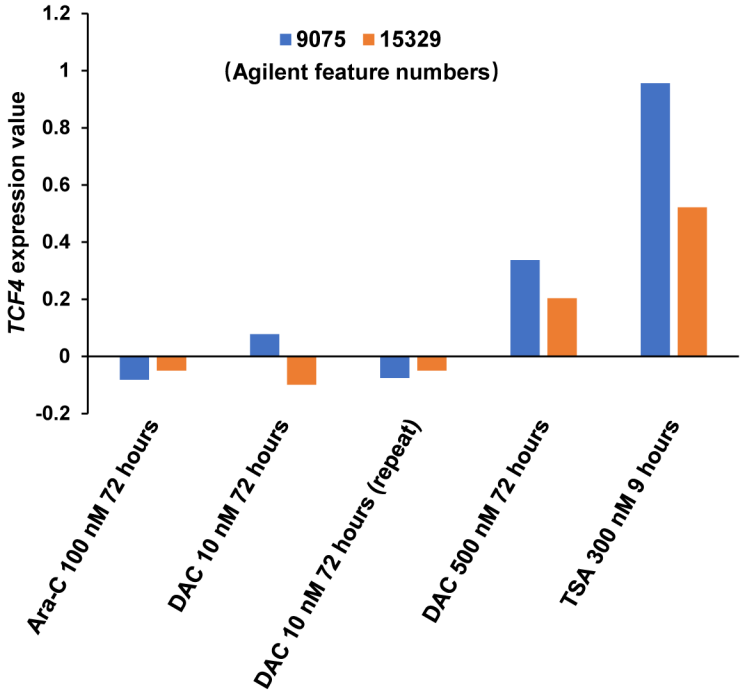

Fig. S3. Upregulation of *E2-2* mRNA in Kasumi-1 cells by DAC and TSA treatments. Microarray-based gene expression data of Kasumi-1 cells under indicated treatments were obtained from Tsai et al., 2012, and were analyzed by the GEO2R program (https://www.ncbi.nlm.nih.gov/geo/geo2r/). Note that DAC and TSA at relatively high dosages (500 and 300 nM, respectively) exhibit consistent effects on upregulation of *TCF4*/*E2-2*. In contrast, Ara-C and a low dosage of DAC (10 nM) have no effect, as the *TCF4*/*E2-2* mRNA levels in these cells are around or under the base line of the expression value. 9075 and 15329 are two Agilent feature numbers that represent the *TCF4*/*E2-2* gene.

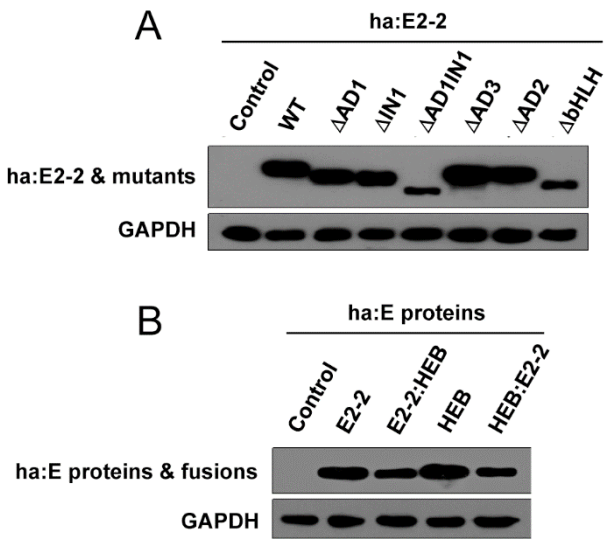

Fig. S4. Western blot results showing proper expression of the E2-2 deletion mutants (*A*) and E2-2 fusions (*B*). 293T cells were transfected with plasmids containing indicated HA-tagged proteins and cell lysates were analyzed with antibodies for HA and GAPDH.

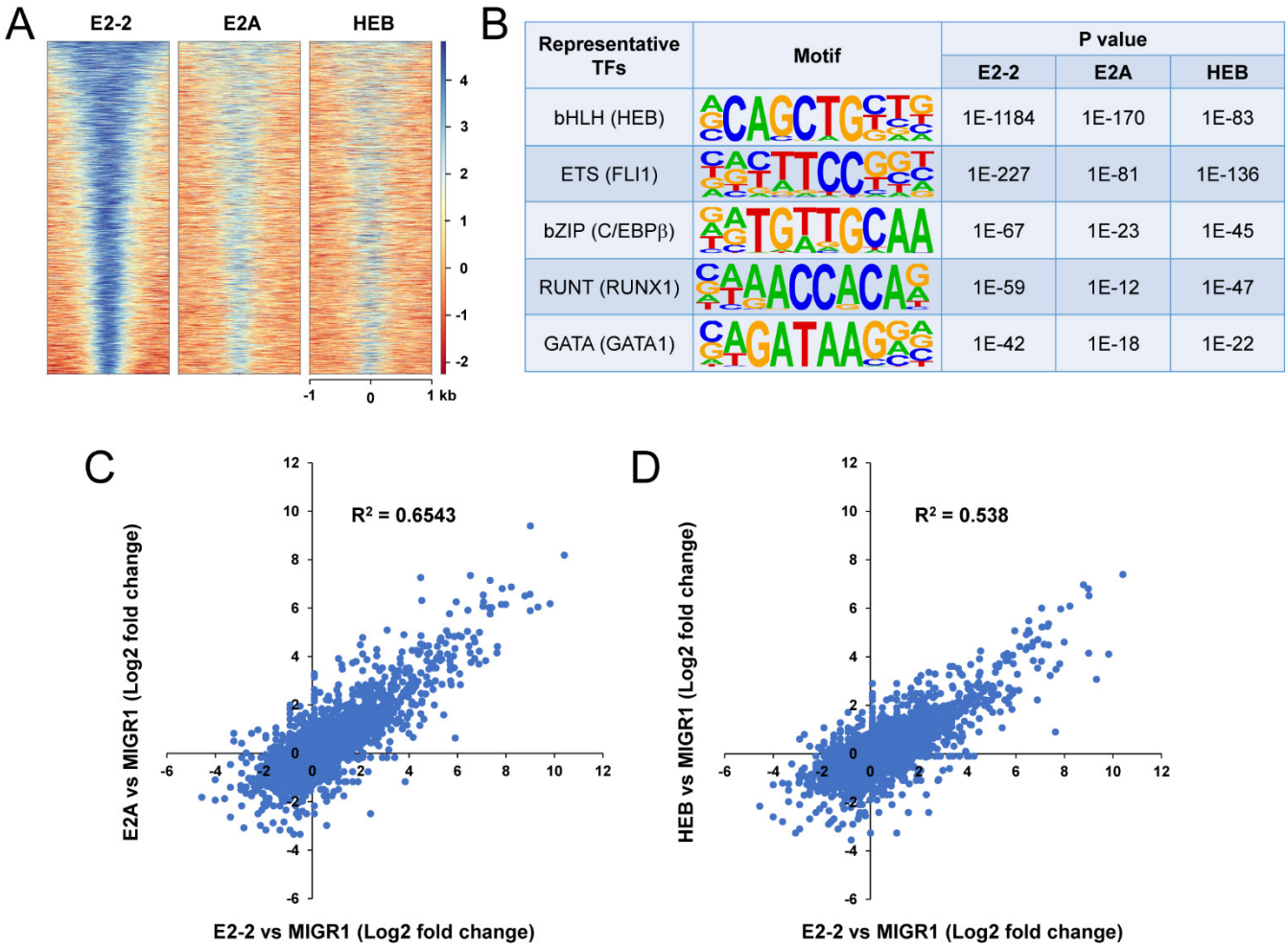

Representative TFs	Motif	P value		
		E2-2	E2A	HEB
bHLH (HEB)		1E-1184	1E-170	1E-83
ETS (FLI1)		1E-227	1E-81	1E-136
bZIP (C/EBPβ)		1E-67	1E-23	1E-45
RUNT (RUNX1)		1E-59	1E-12	1E-47
GATA (GATA1)		1E-42	1E-18	1E-22

Fig. S5. Overlapping functions of E2-2, E2A and HEB in binding to the genome and regulating gene expression. (*A*) Heat map of enrichment scores for E2-2, E2A and HEB on genomic regions from -1 to 1 kb surrounding the E2-2 peaks, ordered by E2-2 binding strength. The top 3000 E2-2 binding sites are shown. (*B*) Top 5 overrepresented transcription factor binding sites (TFBSs) in the binding regions of E2-2, E2A and HEB. Note that the top 5 TFBSs are shared by the three E proteins, although their ranks based on the P values are slightly different. (*C* and *D*) Correlation analyses of the genes regulated by E2-2, E2A and HEB, based on RNA-seq data for Kasumi-1 cells overexpressing E2-2, E2A or HEB versus the negative control (MIGR1).

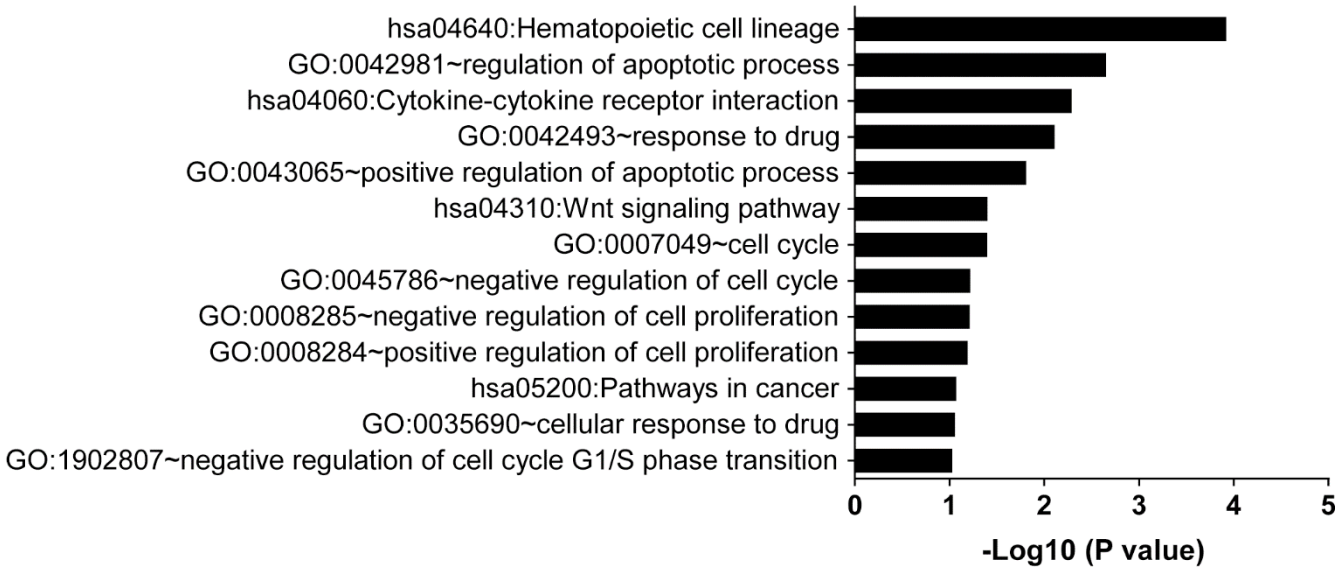

Fig. S6. Gene Ontology (GO) analysis of genes differentially expressed upon E2-2 overexpression. Note that the gene sets of hematopoietic cell lineage and regulation of apoptotic processes are most significantly enriched.

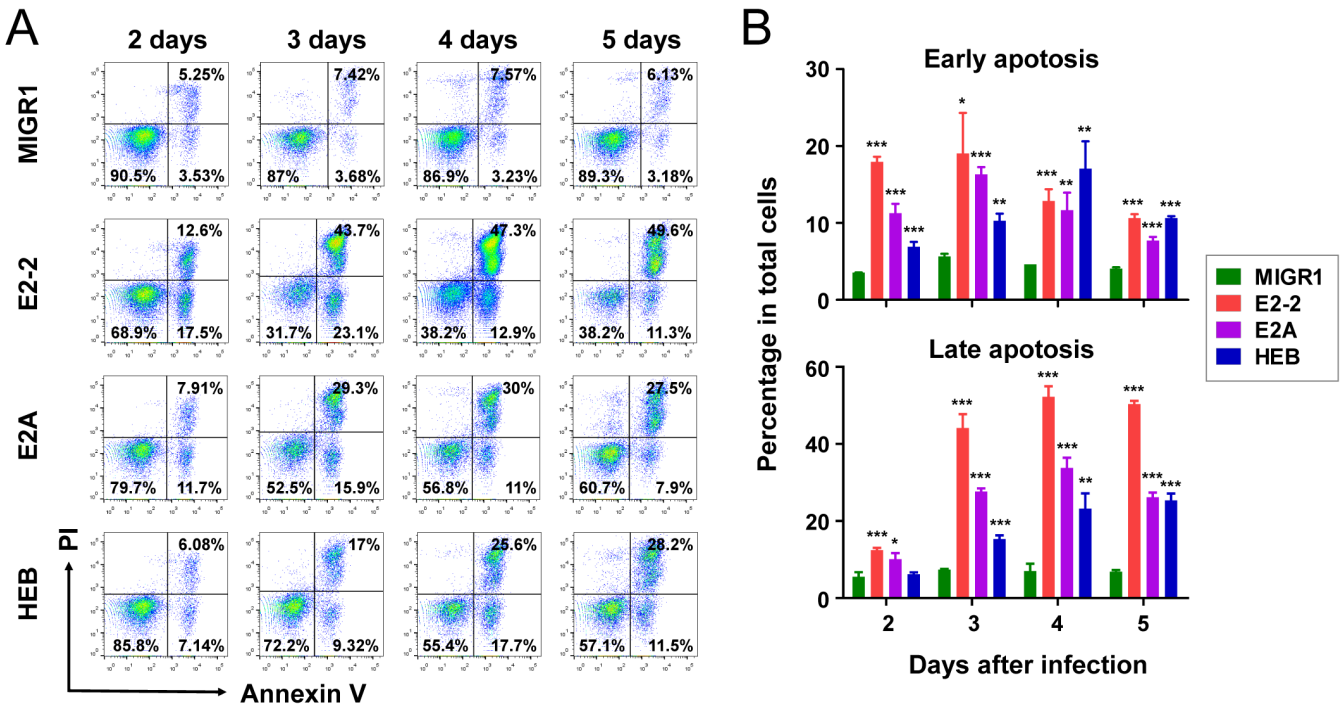

Fig. S7. Analyses of apoptosis of Kasumi-1 cells induced by overexpression of E proteins. (*A*) Representative flow cytometry analysis of apoptotic cells at different time phases after virus infection. (*B*) Quantification of the percentages of early apoptotic (annexin-V$^+$/PI$^-$) and late apoptotic (annexin-V$^+$/PI$^+$) cells. Note that E2-2 shows a most dramatic effect in induction of apoptosis. Data are presented as mean ± SD of triplicate experiments. ***P < 0.001; **P < 0.01; *P < 0.05.

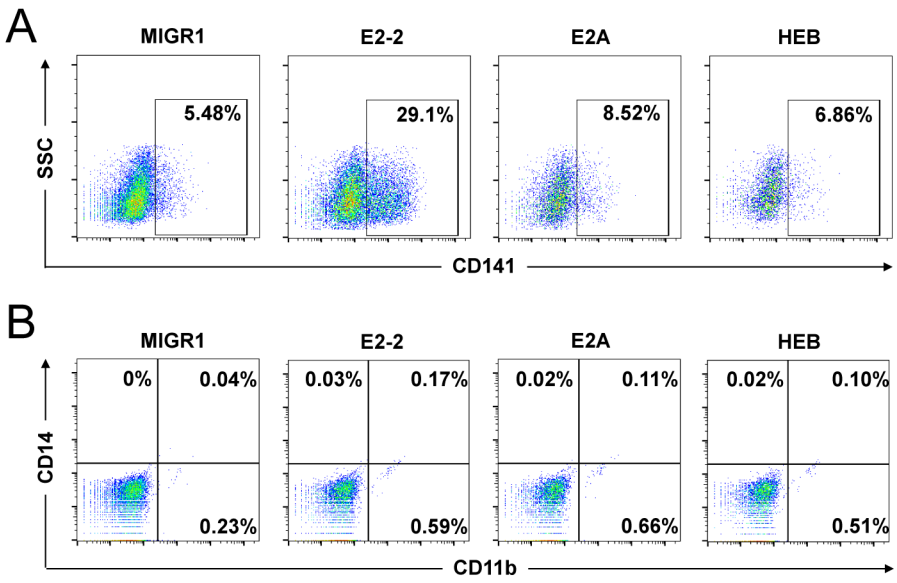

Fig. S8. Overexpression of E2-2 in Kasumi-1 cells induces dendritic, but not myeloid, differentiation. (*A*) Cells were cultured in basic medium for 2 days and the dendritic marker CD141 was measured by flow cytometry. (*B*) The granulocytic marker CD11b and the monocytic marker CD14 were not induced by the three E proteins in Kasumi-1 cells.

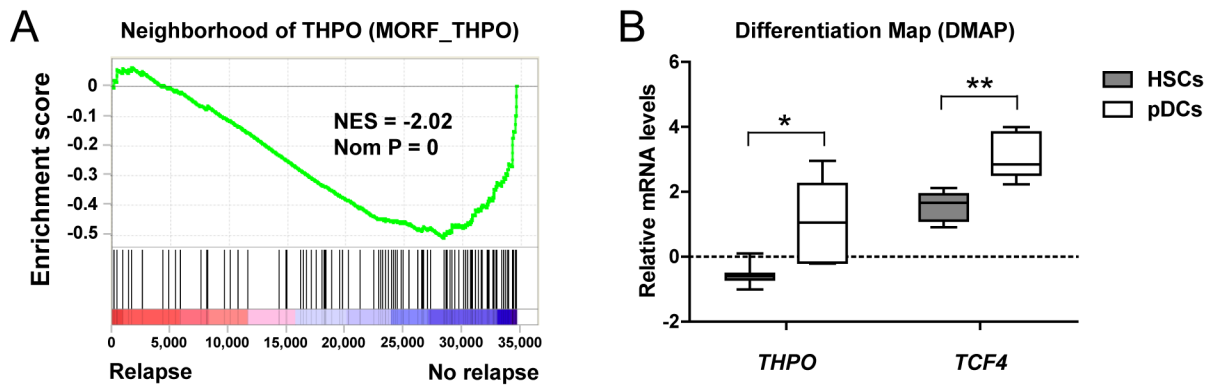

Figure S9. Gene expression profiling and correlation analyses of *THPO* and *E2-2* in t(8;21) AML patient samples and normal hematopoietic cells. (*A*) GSEA of RNA-seq data of t(8;21) AML patient samples indicating a strong correlation of the Neighborhood of THPO gene set (MORF_THPO) with the genes that are relatively specific for the non-relapse patients. (*B*) Relative expression levels of *THPO* and *TCF4*/*E2-2* mRNAs in purified human HSCs and plasmacytoid dendritic cells (pDCs). Note that *THPO* and *TCF4*/*E2-2* are cooperatively upregulated during the differentiation of HSCs to pDCs, and that the *THPO* expression level is extremely low in the HSCs. Data were derived from the Differentiation Map (DMAP) Portal of the Broad Institute. $^{**}P < 0.01$; $^{*}P < 0.05$.

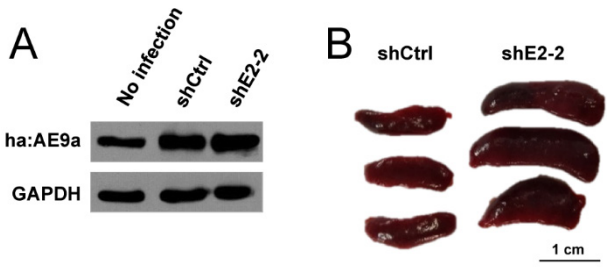

Fig. S10. Knockdown of E2-2 in the AML1-ETO9a–driven leukemia mouse model enhances leukemogenesis. (*A*) Western blot showing that knockdown of E2-2 does not affect the protein level of AML1-ETO9a in leukemic cells. (*B*) Representative images of the larger spleens in the mice harboring E2-2 knockdown leukemic cells relative to those with control cells.

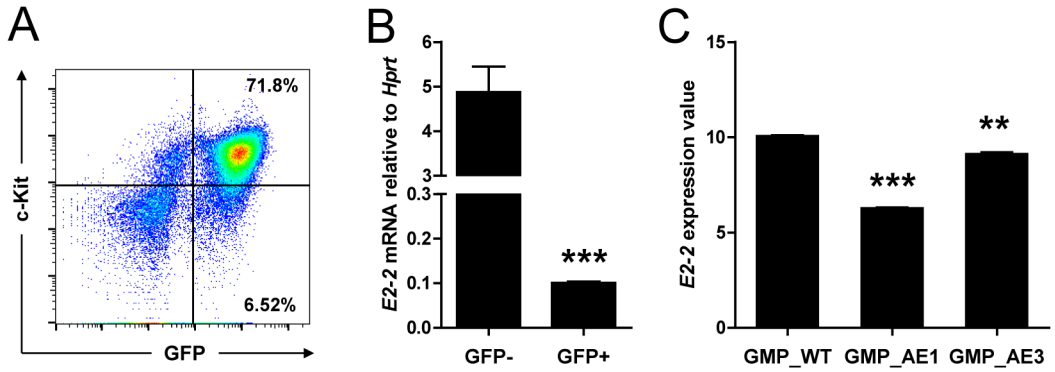

Fig. S11. Suppression of E2-2 in the leukemic cells of two mouse models of t(8;21) AML. (*A*) Flow cytometry analysis of the spleen cells of a leukemic mouse transplanted with AML1-ETO9a–expressing fetal liver HSPCs. (*B*) RT-qPCR analysis of the purified leukemic (GFP^+) and non-leukemic (GFP^-) cells shown in (A). Note that the *E2-2* mRNA expression is significantly decreased in the leukemic cells. Data are presented as mean ± SD of triplicate reactions. (*C*) Decreased expression of *E2-2* in the leukemic cells of a mouse model that is generated by expression of AML1-ETO in the HSPCs of a *Tet2* deficient mouse. Date were obtained from Rasmussen et al., 2015, in which microarray analysis was performed with purified GMPs of two leukemic mice (AE1 and AE3) and a control (WT) mouse. Data are presented as mean ± SD of triplicate experiments of each mouse. ***$P < 0.001$; **$P < 0.01$.

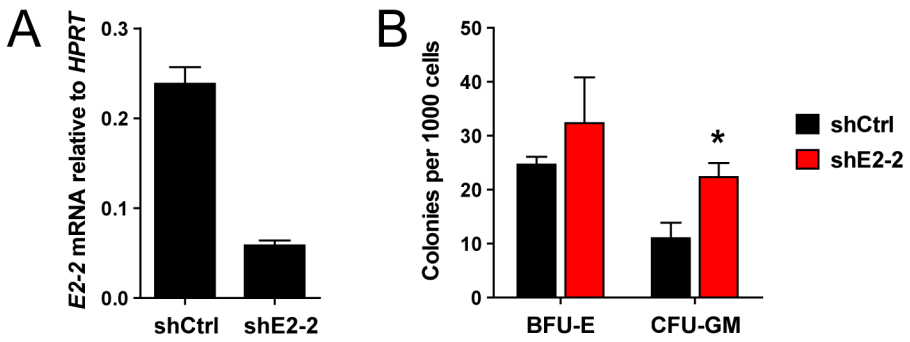

Fig. S12. Role of E2-2 in human normal HSPCs. (A) shRNA-mediated knockdown of E2-2 in human CD34$^+$ HSPCs. Data are presented as mean ± SD of triplicate reactions. (B) Slightly increased capacity of the E2-2–knockdown HSPCs to form myeloid colonies. Data are presented as mean ± SD of triplicate experiments. *$P < 0.05$.